MRF AND DEMPSTER-SHAFER THEORY FOR SIMULTANEOUS SHADOW/VEGETATION DETECTION ON HIGH RESOLUTION AERIAL COLOR IMAGES

Tran-Thanh Ngo, Christophe Collet, Vincent Mazet

iCube, University of Strasbourg, CNRS
300 Bd Sébastien Brant - CS 10413 - 67412 Illkirch, France

ABSTRACT

This paper presents a new method for *simultaneously* detecting shadows and vegetation in remote sensing images, based on Otsu's thresholding method and Dempster-Shafer (DS) fusion which aims at combining different shadow indices and vegetation indices in order to increase the information quality and to obtain a more reliable and accurate segmentation result. The DS fusion is carried out pixel by pixel and is incorporated in the Markovian context while obtaining the optimal segmentation with the energy minimization scheme associated with the MRF. This new approach is applied on remote sensing images and demonstrates its efficiency.

Index Terms— Dempster-Shafer theory, multivariate segmentation, shadow indices, vegetation indices, Markov random field, remote sensing

1. INTRODUCTION

In recent years, the effects of natural catastrophes and human activities have emphasized the need for developing a broader view of the Earth. According to cartographic experts, shadow and vegetation can provide additional geometric and semantic clues about the state of buildings after natural catastrophes. This work is devoted to simultaneous shadow/vegetation detection. Since the shape features of buildings are extracted from this detection, correctness and precision of the segmentation are strongly required.

On the one hand, shadow occurs when objects totally or partially occlude the direct light projected from a source of illumination. Several publications have appeared in recent years documenting shadow detection for aerial images [1–7]. Recent existing shadow detection methods are commonly based on the assumption that regions under shadow become darker but retain their chromaticity. Thus, shadow regions can be detected by choosing a color space with better separation between chromaticity and intensity than the RGB color space (eg. HSV [4], $c_1c_2c_3$ [5], YUV [6], normalised RGB [6]), or a

combination of them [7]. Other authors exploit the properties of shadows, in which shadow regions in the general exhibit lower radiance values over the entire spectrum, and sensor irradiation from shadow regions decreases from short to long wavelengths due to scattering [8]. Based on these assumptions, different shadow indices have been proposed [1, 3, 9]. Most of these methods are simple to implement and computationally inexpensive. However, because they make comparisons at the pixel-level, they are susceptible to noise. They also fail to exploit image geometric information, lead to typically unsatisfactory performance for real complex images.

On the other hand, vegetation indices have been used extensively to estimate the vegetation density from aerial and satellite images for many years. Beside the so-called Normalized Difference Vegetation Index (NDVI) which is very popular in vegetation detection [10], [11], different kinds of vegetation indices which utilize only the red, green and blue spectral bands have been proposed in the literature. Among them, color index of vegetation extraction (CIVE) [12], excess green index (ExG) [13], and excess green minus excess red (ExGR) [14] are used. The advantages of using these indices is that they accentuate a particular color such as plant greenness, which should be intuitive for human comparison [15]. Moreover, they do not require the near-infrared band, which is not available for RGB color images, such as NDVI. Different tests of these indices can be found in [13, 15].

Current shadow/vegetation detection methods in the literature detect separately shadow regions and vegetation regions [16], [17]. The drawback of these methods is that, for example, a vegetated pixel covered by shadow can be classified as vegetation (by a vegetation detection algorithm), and at the same time as shadow (by a shadow detection algorithm). Thus, these methods can not provide a sufficiently good segmentation map. In fact, visual inspection also has a similar problem since the pixel information is imprecise and uncertain. In this paper, we propose a new method of simultaneously detecting shadow regions and vegetation regions, in other words, segmenting images into three classes: shadow, vegetation and other. Each feature image computed from shadow index or vegetation index can be considered as an information source. In this context, Dempster-Shafer (DS) fusion [18, 19] that aims at merging different data sources is

employed. The principal advantage of this theory is its ability to take into account ignorance of the information by affecting a degree of confidence which is called a mass function to all simple and compound hypotheses. However, since this isolates pixel by pixel use, assuming that each pixel is independent of its neighbors and does not take into account spatial dependencies, the performance of the DS fusion is sensitive to noise. The Markov Random Field (MRF) [20] is thus employed to incorporate spatial information into the image.

This approach differs from what can be found in the literature in three distinct aspects: firstly, it introduces a new scheme to *simultaneously* detect shadow regions and vegetation regions. Secondly, the use of DS theory allows us to combine different shadow indices and vegetation indices in order to increase the information quality and to obtain a more reliable and accurate shadow/vegetation detection. Thirdly, we exploit image geometric information by using a Markov random field, that is often used in image segmentation but rarely in the shadow/vegetation detection case.

The remaining paper is organized as follows. In section 2, we introduce the shadow index and vegetation index which are employed. The theory of evidence and its application in shadow/vegetation detection is described in Section 3. Section 3.2 outlines the link between MRF and DS fusion. The experimental results are reported in Section 4, and the paper is concluded in Section 5.

2. PHOTOMETRIC INVARIANT COLOR MODELS

We propose exploiting the common assumptions made on shadows [8], using the shadow indices proposed in the literature [1–7]. The behaviour of these shadow indices have been evaluated and the best results are obtained using the c_3 component of the $c_1 c_2 c_3$ color space [21]. The c_3 component has been successfully used to detect shadow regions in [2,22], and defined as follows: $c_3 = \arctan\left(\dfrac{B}{\max(R, G)}\right)$ for R,G and B representing respectively the red, green and blue color components in the image. One of the problems though when using the c_3 index is its instability for certain color values that lead to the misclassification of non-shadow pixels as shadow (false positives) [2, 22]. Then, we propose to combine luminance L (HSL color space) and c_3 to detect shadow regions as proposed in [23] even if luminance L detects the areas which includes shadows *and* vegetation. For vegetation detection, among different vegetation indices presented in [15], of remarkable effectiveness is the excess green ExG, one of the most famous agronomic contrasts defined by [13] as follows: $\text{ExG} = \dfrac{2 \times G - R - B}{R + G + B}$.

3. THEORY OF EVIDENCE

Dempster-Shafer theory (DS) is a mathematical theory of evidence. This theory was developed by A.P Dempster [18] and G. Shafer [19] and often described as a generalization of the Bayesian theory to represent information that is inaccurate and uncertain at the same time.

3.1. Use of DS Evidence Theory for shadow/vegetation detection

Given the (R,G,B) color representation of a pixel, we use c_3 to build Y_1, ExG to build Y_2, L to build Y_3. Let us denote $\omega_1, \omega_2, \omega_3$, three clusters representing respectively "shadow", "vegetation" and "other". Our algorithm takes three feature images Y_1, Y_2, Y_3 as the input, and the output is a segmented image X, where values of X are in $\Omega = \{\omega_1, \omega_2, \omega_3\}$.

The automatic thresholding technique proposed by Otsu [24] is applied over the image Y_1, Y_2, Y_3 for determining the optimal threshold to extract respectively shadow regions [1, 3], vegetation regions and dark regions (that may include shadow regions and vegetation regions). After thresholding, image Y_1 (resp. Y_2 ; Y_3) is segmented into two classes ω_1 and $\{\omega_2, \omega_3\}$ (resp. ω_2 and $\{\omega_1, \omega_3\}$; $\{\omega_1, \omega_2\}$ and ω_3). DS theory for image segmentation allows us to fuse one by one the pixels from the three images Y_1, Y_2, Y_3 and to infer simple hypotheses H_i representing individual cluster: $H_i = \{\omega_i\}$, A_i designating either simple hypotheses H_i or a union of simple hypotheses. The frame of discernment is $\Theta = \{\{\omega_1\}, \{\omega_2\}, \{\omega_3\}\}$.

The method of generating mass functions is based on the assumption of Gaussian distributions [25]. The mass function for image Y_1, defining on $\{\emptyset, A_1, A_2, \Theta\}$, where $A_1 = \{\omega_1\}$, $A_2 = \{\{\omega_2\}, \{\omega_3\}\}$, is estimated as follows:

$$m_1(A_i) = \frac{1}{\sigma_{1i}\sqrt{2\pi}} \exp\left(-\frac{(y_{1s} - \mu_{1i})^2}{2\sigma_{1i}^2}\right) \quad (1)$$

Here, $i \in \{1, 2\}$, y_{1s} is the value of the considered pixel s (in image Y_1). μ_{1i} (resp. σ_i^2) represents the mean (resp. the variance) of pixels with hypothesis A_i present in Y_1. They are respectively estimated by $\mu_{1i} = \frac{1}{|A_i|}\sum_{s \in A_i} y_{1s}$, $\sigma_{1i}^2 = \frac{1}{|A_i|-1}\sum_{s \in A_i}(y_{1s} - \mu_{1i})^2$ where $\mid A_i \mid$ denotes the number of pixels verifying A_i.

The advantage of DS theory lies in representing uncertainty by means of belief on the whole frame of discernment. This basic belief assignment allows defining $m_1(\Theta)$ with the following equation: $m_1(\Theta) = (1 - m_1(A_1)) \times (1 - m_1(A_2))$. These mass functions are then normalized so that their sum is equal to 1. The mass functions for image Y_2, defining on $\{\emptyset, \{\omega_2\}, \{\{\omega_1\}, \{\omega_3\}\}, \Theta\}$ and the mass functions for Y_3, defining on $\{\emptyset, \{\{\omega_1\}, \{\omega_2\}\}, \{\omega_3\}, \Theta\}$ are estimated in the same way. Once the mass function of the three images are estimated, their combination is performed using the orthogonal

sum :

$$m = m_1 \oplus m_2 \oplus m_3 \qquad (2)$$

with $\oplus$ is the sum of DS orthogonal rule [18]. The decisional procedure consists in choosing the maximum plausibility, the maximum belief or the pignistic probability as being the most likely hypothesis H_i [18]. Decision-making is carried out on simple hypotheses which represent the classes in the images.

3.2. Markov Random Field Modeling

The DS fusion processes at a pixel-level, assumes that each pixel in the image is independent of its neighbors and does not take into account spatial dependencies. Thus, the performance of the DS fusion is highly sensitive to noise. To overcome this shortcoming, the MRF [26] may be employed, to consider not only the measurements at the pixel's location, but also the class values among its closest neighbors. Let X be a random field over the set $\mathcal{S}$ of pixels, taking its values from a finite set of classes $\Omega = \{\omega_1, \ldots, \omega_K\}$ and x a realization of X. x_s denotes the value of x at the pixel $s \in \mathcal{S}$. x_s is a realization of the random variable X_s. By definition, X is a Markov random field if and only if $p(X_s = x_s | x_{\mathcal{S}-\{s\}}) = p(x_s | x_{\mathcal{V}_s})$ where $\mathcal{V}_s$ is the set of sites neighboring s.

Given the observed images $\mathbf{y} = (y_1, \ldots, y_m)$, the segmented image x can be obtained using the MAP estimate of X. Thus,

$$
\begin{aligned}
\hat{x}_{\text{MAP}} &= \arg\max_x \{P(X = x | \mathbf{Y} = \mathbf{y})\} \\
&= \arg\min_x \{-\log(p(\mathbf{y}|x)) - \log(p(x))\}
\end{aligned} \qquad (3)
$$

This problem can be solved by the iterative conditional models (ICM) algorithm [20]. In this method, a raster scan is used to iteratively visit all the pixels in field X. We denote $\hat{x}_{\mathcal{S}-\{s\}}$ as a provisional estimate of the segmentation field everywhere except at location s. Given the data $\mathbf{y}$ and the current segmentation $\hat{x}_{\mathcal{S}-\{s\}}$, the algorithm updates the current segmentation $\hat{x}_s$ at pixel s, and replaces it with the new value $\hat{x}_s$ which maximizes $P(x_s | \mathbf{y}, \hat{x}_{\mathcal{S}-\{s\}})$ with respect to x_s. Since we consider X as an MRF, the latter follows from Bayes' theorem that

$$P(x_s | \mathbf{y}, \hat{x}_{\mathcal{S}-\{s\}}) = p(\mathbf{y}_s | x_s) p(x_s | \hat{x}_{\mathcal{V}_s}) \qquad (4)$$

Given this second-order neighborhood, where the prior probability term in Eq. 4 can be assigned using

$$p(x_s | \hat{x}_{\mathcal{V}_s}) = \frac{e^{-\beta \sum_{l \in \mathcal{V}_s} \{1 - \delta(x_s, \hat{x}_l)\}}}{\sum_{x_s \in \Omega} e^{-\beta \sum_{l \in \mathcal{V}_s} \{1 - \delta(x_s, \hat{x}_l)\}}} \qquad (5)$$

where $\delta(\cdot)$ stands for the Kronecker's delta function.

3.3. DS Theory in Markovian Context

In recent years, both the MRF and DS theory of evidence have been incorporated into more general methods for scene classification, often involving multisource analysis [27–29]. In fact, the probabilistic framework assigns likelihood values $p(y_s | x_s)$ only for each class $\omega_i \in \Omega$. From the view of evidence theory, the likelihood can be assimilated to a mass function which charges the singleton $H_{x_s} = \{\omega_i\}$. In [29], the authors proposed replacing the likelihood term in Eq. (4) by the plausibility function to take into account all information contained in single and compound hypothesis, as follows:

$$p(y_s | x_s) \equiv Pls_s(H_{x_s}) = \sum_{A_i \cap H_{x_s} \neq \emptyset} m_s(A_i) \qquad (6)$$

For each pixel s, the mass function $m_s(A_i)$ is computed by using Eq. (2). And the conditional probability in Eq. (5) which assigns values to single hypotheses can be replaced by:

$$m_s(A_i | \hat{x}_{\mathcal{V}_s}) = \frac{e^{-\sum_{H_k \cap A_i \neq \emptyset} \beta \sum_{l \in \mathcal{V}_s} \{1 - \delta(\omega_k, \hat{x}_l)\}}}{\sum_{A_j \subset \Theta} e^{-\sum_{H_k \cap A_j \neq \emptyset} \beta \sum_{l \in \mathcal{V}_s} \{1 - \delta(\omega_k, \hat{x}_l)\}}} \qquad (7)$$

to deal with the compound hypotheses $A_i \subset \Theta$.

Considering the likelihood and the conditional membership components in Eqs. (6) and (7) as two "evidential" sources of information, the Dempster-Shafer orthogonal rule is used to combine these two sources of information. The posterior probability in Eq. (4) can be replaced using $M_s(.)$, which carries the joint information.

$$M_s(A_i) = \frac{1}{1 - \mathcal{K}} \sum_{Ap \cap Aq = A_i} m_s(A_p) m_s(A_q | \hat{x}_{\mathcal{V}_s}) \qquad (8)$$

where $\mathcal{K} = \sum_{Ap \cap Aq = \emptyset} m_s(A_p) m_s(A_q | \hat{x}_{\mathcal{V}_s})$. Once all of the mass function of the single and compound hypotheses related to pixel s are determined, several approaches can be chosen for the estimation of $\hat{x}_s$, for example, by maximizing the plausibility function :

$$\hat{x}_s = \arg\max_{x_s} \left(\sum_{A_i \cap H_{x_s} \neq \emptyset} M_s(A_i) \right)$$

4. EXPERIMENTAL RESULTS

The proposed iterative data fusion method takes as input three feature images c_3, ExG, and L, resulting in a segmented image X with labels in { "shadow", "vegetation", "other"}. The shadow/vegetation detection method using Otsu's thresholding approach and data fusion technique, called THDS, is used as the initialization of our algorithm. Through iterations, we obtain the final shadow/vegetation detection result. We compare the proposed method with the shadow detection method based on Otsu's thresholding technique, the vegetation detection method based on Otsu's thresholding technique and the THDS method. Comparative experimental results are shown in Fig. 1 and Table 1.
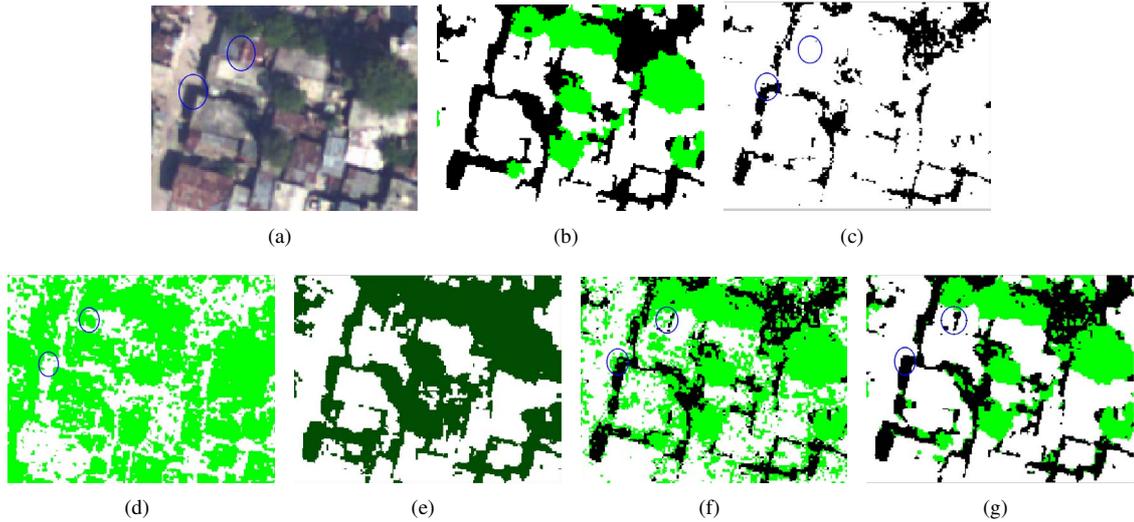
Fig. 1. (a) RGB remote sensing image of urban areas, (b) the manually interpreted shadow masks (black areas) and vegetation masks (green areas) as ground truth of shadow regions and vegetation regions respectively, (c) shadow detection (SD) by Otsu's method, (d) vegetation detection (VD) by Otsu's method, (e) dark (shadow + vegetation) detection by Otsu's method with luminance L, (f) The THDS method, and (g) The proposed method. We observe that the proposed method solves the problems of false dismissals, and improves the accuracy of segmentation. The fusion corrects the misclassification of each feature, and the ICM removes the small objects in segmentation. The shape of shadow regions is precisely obtained since the image geometric information is exploited through MRF modelling (blue circles).

Method	Shadow detection					Vegetation detection				
	Producer's accuracies		User's accuracies		Overall accuracy	Producer's accuracies		User's accuracies		Overall accuracy
	Shadow $P_s(\%)$	Nonshadow $P_n(\%)$	Shadow $U_s(\%)$	Nonshadow $U_n(\%)$	$\tau(\%)$	Vegetation $P_v(\%)$	Nonvegetation $P_v(\%)$	Vegetation $U_v(\%)$	Nonvegetation $U_v(\%)$	$\tau(\%)$
SD	56.53	**99.92**	99.58	86.98	88.81					
VD						92.53	44.83	26.61	96.52	53.31
THDS method	70.68	99.65	**98.59**	90.81	92.24	97.08	73.01	43.74	99.14	77.29
Proposed method	**89.17**	99.19	97.45	**96.38**	**96.63**	**99.11**	**95.75**	**83.47**	**99.80**	96.35

Table 1. Shadow/vegetation detection accuracy measurements of the image in Fig. 1. In this work, we adopt the same metrics and accuracy table from [1] and [8]. The evaluation metrics are defined based on true positive (TP), false negative (FN), false positive (FP), true negative (TN). Concerning shadows (for vegetation detection, these parameters are defined in the same way), TP is the number of shadow pixels correctly identified, FN is the number of shadow pixels identified as non-shadow, FP is the number of non-shadow pixels identified as shadows and TN is the number of non-shadow pixels correctly identified. The sum TP + FN + FP + TN stands for the total number of pixels in the image. Among these metrics, the producer's accuracies (also known as recall) indicate how well pixels of known categories are correctly classified. The user's accuracies (also known as precision) indicate the probabilities of pixels being correctly classified into actual categories on the ground. Combining the accuracies of the user and the producer, the overall accuracy τ can be used to evaluate the correctness percentage of the algorithm. For a good algorithm, values of these metrics should be high.

From the aforementioned three types of accuracy, Table 1 shows the accuracy comparison for shadow detection using Otsu's method, vegetation detection using Otsu's method, the THDS method and our proposed method. It is shown that the accuracy of our proposed method is high and through iterations, the ICM provides better accuracy performance compared with the THDS method.

5. CONCLUSION

This paper presents a novel shadow/vegetation detection strategy based on a fusion procedure whose goal is to manage the imprecision and uncertainty of a pixel's information concerning shadow and vegetation. On the other hand, this fusion procedure also makes it possible to combine different shadow index c_3, vegetation index ExG and the luminance L. The spatial correlation between neighboring pixels is also taken into account using the MRF modelling in order to finally obtain a more reliable and efficient segmentation map with good accuracy, which is demonstrated in the experimental results. This method has the interest in extending for combining other invariant color features. For example, if image has the NIR bands, the use of NDVI vegetation index may detect better vegetation, and since sensor radiance received from shadowed regions decreases from short to long wavelengths due to scattering, it is easier to distinguish shadows from non-shadows with NIR channels rather than visible channels [8].

6. REFERENCES

[1] Victor J.D.Tsai, "A comparative study on shadow compensation of color aerial images in invariant color models," *IEEE Transactions on Geoscience and Remote Sensing*, vol. 44, no. 6, pp. 1661–1671, June 2006.

[2] V. Arévalo, J. González, and G. Ambrosio, "Shadow detection in colour high-resolution satellite images," *International Journal of Remote Sensing*, vol. 29, no. 7, pp. 1945–1963, 2008.

[3] Kuo-liang Chung, Yi-ru Lin, and Yong-huai Huang, "Efficient shadow detection of color aerial images based on successive thresholding scheme," *IEEE Transactions on Geoscience and Remote Sensing*, vol. 47, no. 2, pp. 671–682, Feb. 2009.

[4] Rita Cucchiara, Costantino Grana, Massimo Piccardi, and Andrea Prati, "Detecting moving objects, ghosts, and shadows in video streams," *IEEE Transactions on Pattern Analysis and Machine Intelligence*, vol. 25, no. 10, pp. 1337–1342, 2003.

[5] Elena Salvador, Andrea Cavallaro, and Touradj Ebrahimi, "Cast shadow segmentation using invariant color features," *Computer Vision and Image Understanding*, vol. 95, no. 2, pp. 238–259, Aug. 2004.

[6] Chun-Ting Chen, Chung-Yen Su, and Wen-Chung Kao, "An enhanced segmentation on vision-based shadow removal for vehicle detection," in *International Conference on Green Circuits and Systems*, 2010, pp. 679–682.

[7] Bangyu Sun and Shutao Li, "Moving cast shadow detection of vehicle using combined color models," in *Chinese Conference on Pattern Recognition*, 2010, pp. 1–5.

[8] K.R.M. Adeline, M. Chen, X. Briottet, S.K. Pang, and N. Paparoditis, "Shadow detection in very high spatial resolution aerial images: A comparative study," *ISPRS Journal of Photogrammetry and Remote Sensing*, vol. 80, pp. 21–38, 2013.

[9] Airton M.Polidorio, "Automatic shadow segmentation in aerial color images," *Computer Graphics and Image Processing, 2003. SIBGRAPI 2003. XVI Brazilian Symposium*, pp. 270–277, 2003.

[10] JW Rouse, RH Haas, JA Schell, DW Deering, and JC Harlan, *Monitoring the vernal advancement and retrogradation (greenwave effect) of natural vegetation*, Texas A & M University, Remote Sensing Center, 1974.

[11] Compton J Tucker, "Red and photographic infrared linear combinations for monitoring vegetation," *Remote sensing of Environment*, vol. 8, no. 2, pp. 127–150, 1979.

[12] T. Kataoka, T. Kaneko, H. Okamoto, and S. Hata, "Crop growth estimation system using machine vision," in *Proceedings of the 2003 IEEE/ASME International Conference on Advanced Intelligent Mechatronics*, 2003, pp. 1079–1083.

[13] D. M. Woebbecke, G. E. Meyer, K. Von Bargen, and D. A. Mortensen, "Color indices for weed identification under various soil, residue, and lighting conditions," *Transactions of the ASAE*, vol. 38, no. 1, pp. 259–269, 1995.

[14] J.C. Neto, G.E. Meyer, and D.D. Jones, "Individual leaf extractions from young canopy images using Gustafson–Kessel clustering and a genetic algorithm," *Computers and Electronics in Agriculture*, vol. 51, pp. 66–85, 2006.

[15] George E. Meyer and João Camargo Neto, "Verification of color vegetation indices for automated crop imaging applications," *Computers and Electronics in Agriculture*, vol. 63, no. 2, pp. 282–293, Oct. 2008.

[16] Nicholas Shorter and Takis Kasparis, "Automatic vegetation identification and building detection from a single nadir aerial image," *Remote Sensing*, vol. 1, no. 4, pp. 731–757, Oct. 2009.

[17] Ali Ozgun Ok, "Automated detection of buildings from single vhr multispectral images using shadow information and graph cuts," *ISPRS Journal of Photogrammetry and Remote Sensing*, vol. 86, pp. 21–40, Dec. 2013.

[18] Arthur P Dempster, "A generalization of Bayesian inference," *Journal of the Royal Statistical Society. Series B (Methodological)*, pp. 205–247, 1968.

[19] Glenn Shafer, *A mathematical theory of evidence*, vol. 1, Princeton university press Princeton, 1976.

[20] Julian Besag, "On the statistical analysis of dirty picture," *Journal of the Royal Statistical Society*, vol. 48, no. 3, pp. 259–302, 1986.

[21] Theo Gevers and Arnold W M Smeulders, "Color-based object recognition," *Pattern recognition*, vol. 32, no. 3, pp. 453–464, 1999.

[22] E. Salvador, A. Cavallaro, and T. Ebrahimi, "Shadow identification and classification using invariant color models," in *IEEE International Conference on Acoustics, Speech, and Signal Processing*. 2001, vol. 3, pp. 1545–1548, IEEE.

[23] Jian Yao and Zhonefei (Mark) Zhang, "Hierarchical shadow detection for color aerial images," *Computer Vision and Image Understanding*, vol. 102, no. 1, pp. 60–69, 2006.

[24] Nobuyuki Otsu, "A threshold selection method from gray-level histograms," *Automatica*, vol. 11, no. 285-296, pp. 23–27, 1975.

[25] S Ben Chaabane, M Sayadi, F Fnaiech, and E Brassart, "Color image segmentation based on Dempster-Shafer evidence theory," in *Electrotechnical Conference, 2008. MELECON 2008. The 14th IEEE Mediterranean*. IEEE, 2008, pp. 862–866.

[26] S Geman and D Geman, "Stochastic relaxation, Gibbs distributions, and the Bayesian restoration of images," *IEEE Transactions on Pattern Analysis and Machine Intelligence*, vol. 6, no. 6, pp. 721–41, 1984.

[27] Azzedine Bendjebbour, Yves Delignon, L. Fouque, V. Samson, and W. Pieczynski, "Multisensor image segmentation using Dempster-Shafer fusion in Markov fields context," *IEEE Transactions on Geoscience and Remote Sensing*, vol. 39, no. 8, pp. 1789–1798, 2001.

[28] Samuel Foucher, Mickaël Germain, and Jean-Marc Boucher, "Multisource classification using ICM and Dempster–Shafer theory," *IEEE Transactions on Instrumentation and Measurement*, vol. 51, no. 2, pp. 277–281, 2002.

[29] Layachi Bentabet and Jiang Maodong, "A combined Markovian and Dirichlet sub-mixture modeling for evidence assignment: Application to image fusion," *Pattern Recognition Letters*, vol. 29, no. 13, pp. 1775–1783, 2008.